Biophysical Chemistry 42 (1992) 13–21
Elsevier Science Publishers B.V., Amsterdam

BIOCHE 01618

Simulation of the time course of macromolecular separations in an ultracentrifuge. I. Formation of a cesium chloride density gradient at 25 °C

Allen P. Minton

Laboratory of Biochemical Pharmacology, National Institute of Diabetes, Digestive, and Kidney Diseases, National Institutes of Health, Bethesda, MD 20892 (USA)

(Received 16 April 1991; accepted in revised form 12 June 1991)

Abstract

A method is described for rapid numerical simulation of the time course of the formation of a density gradient of CsCl in an ultracentrifuge at 25 °C. Results of simulations compare well with those of experiments carried out in analytical and preparative ultracentrifuges.

Keywords: Macromolecular separations by ultracentrifugation; Density gradient formation; Thermodynamic properties of CsCl solutions; Hydrodynamic properties of CsCl solutions; Controlled sedimentation; Sedimentation simulation; Centrifuge run optimization

1. Introduction

The preparative ultracentrifuge is widely used to separate and purify different classes of biological macromolecules. Several types of separations have traditionally required many hours of centrifugation at the highest rotor velocities of which a particular centrifuge and rotor are capable. It was felt that a mathematical model that would allow investigators to rapidly simulate the time course of a preparative experiment would be a useful tool for the optimization of planned experiments, conceivably resulting in the savings of considerable amounts of time, valuable chemical and biochemical reagents, and a substantial reduction in mechanical stress and resulting fatigue. The present paper is the first in a series that will document the implementation of one such mathematical model.

The model to be described is based upon an approximate numerical solution of the Lamm (or sedimentation–diffusion) equation in one dimension, for a solution containing two macromolecular species at low concentration and a single low molecular weight density-gradient forming species at high concentration. The sedimentation of the macrosolutes is obviously a sensitive function of the time-dependent distribution of the gradient-forming solute. The sedimentation of the gradient-former is, on the other hand, postulated to be independent of the presence of small amounts of macrosolute, and may be treated as an independent problem. In this first paper a mathematical model describing the sedimentation of one of the

most widely used gradient forming salts, cesium chloride, is presented.

The paper is organized as follows. First, the principles and approximations underlying the simulation are described and justified. The model requires functional descriptions of the dependence of thermodynamic and hydrodynamic properties of CsCl solutions upon concentration over a broad concentration range. Empirical and semi-empirical functions are then introduced and fit to appropriate data from the literature in order to provide the required input. Next, the results of simulations of CsCl density gradient formation and decay under several different sets of experimental conditions are presented and compared with the results of experiment.

2. The simulation model

The transport of the solute species of a binary solution under the influence of a centrifugal field is described by a sedimentation–diffusion equation in one dimension [1]:

$$J = s(w)w\omega^2 r - D(w)\ \mathrm{d}w/\mathrm{d}r \qquad (1)$$

where J is the net outward flux of solute, r is the distance from the axis of rotation, w the weight per volume (w/v) concentration of solute, ω the angular velocity of the rotor, $s(w)$ the sedimentation coefficient, and $D(w)$ the Fickian or mutual coefficient of diffusion. In the limit of low solute concentration, the values of s and D become constant, but, as indicated by the notation, depend in the general case upon solute concentration, and thus vary with time and radial position as well.

In the simulation, the solution within the centrifuge tube or cell is divided into n laminar compartments of equal thickness Δr having $n + 1$ boundaries. The boundaries are numbered 1 to $n + 1$ consecutively, from left to right by convention. The compartments are numbered 1 to n consecutively; each compartment lies directly to the right of the correspondingly numbered boundary. The radial position of the ith boundary is denoted by $r(i)$, such that

$$r(1) \equiv r_{\mathrm{meniscus}}$$

$$r(n+1) \equiv r_{\mathrm{base}}$$

$$\Delta r = [r(n+1) - r(1)]/n$$

$$r(i) = r(1) + (i-1)\ \Delta r$$

To each boundary is assigned a cross-sectional area $A(i)$. For example, if the solution is in a sector-shaped cell,

$$A(i) = \Theta r(i) h$$

where Θ is the sector angle in radians and h is the width of the cell (solution) in the axial direction. If the solution is in a cylindrical tube with inner radius r_t, with the tube axis oriented radially, then

$$A(i) = \pi r_t^2$$

This formulation embodies the first of two major approximations that provide a basis for the present simulation model. A one-dimensional treatment of sedimentation is only strictly valid for a sector-shaped cell, since it is only within such a cell that directed motion of solute and solvents is limited to the radial direction (excluding negligible motions arising from Coriolis forces). Clearly some solute particles moving outward in a radial direction will have a trajectory that intersects the wall of a cylindrical tube during the course of the simulation. Application of a one-dimensional model to a cell geometry that is other than sector-shaped is equivalent to assuming that no significant fraction of solute within a laminar compartment has a local concentration that deviates significantly from the average concentration calculated as described below. In the following papers of this series we shall demonstrate, by comparison with experimental results, that a one-dimensional model can produce useful approximate numerical results for cell geometries, such as the cylindrical tube, in which significant solute motion takes place in other than the radial direction.

The change in solute concentration with time at a particular radial position in the cell is given

by an equation of continuity, expressing the condition of mass conservation:

$$\frac{dw(i)}{dt} = \frac{J(i)A(i) - J(i+1)A(i+1)}{V(i)} \qquad (2)$$

where $w(i)$ is the w/v concentration of solute in the ith compartment (lying to the right of the ith boundary), and $V(i)$ is the volume of the ith compartment, approximated by

$$V(i) = \Delta r \frac{A(i) + A(i+1)}{2} \qquad (3)$$

$J(i)$, the flux outward through the ith boundary, is given by the following approximation to eq. (1):

$$J(i) = \begin{cases} 0 & \text{for } i = 1,\ n+1 \\ s[w_b(i)]\, w_b(i)\, \omega^2 r(i) & \\ \quad -D[w_b(i)]\left(\dfrac{w(i) - w(i-1)}{\Delta r}\right) & \\ \quad \text{for } 2 \le i \le n & \end{cases} \qquad (4)$$

where $w_b(i)$ denotes the concentration of solute at the ith boundary, given by

$$w_b(i) = \frac{w(i-1) + w(i)}{2} \qquad (5)$$

While the use of linear interpolations and approximations to differential quantities limits the accuracy of the simulation, the speed of numerical computation is substantially enhanced relative to that obtained using higher order approximations, and it will be shown that simulations employing the linear approximations yield realistic results over a wide variety of experimental conditions.

A simulation is carried out as follows. First, geometry calculations specifying the values of Δr, $r(i)$, $A(i)$ and $V(i)$ are performed. Then the initial values of $w(i)$, ω, and a parameter Δt, representing the increment of simulated elapsed time between successive iterations of the procedure described below, are specified. Then the following calculations are carried out in an iterative fashion, with the results of the previous iteration being used as input data for the current iteration:

(1) Values of $w_b(i)$ are computed via eq. (5).
(2) The values of $s[w(i)]$ and $D[w(i)]$ are calculated using expressions derived in the following section.
(3) The values of $J(i)$ are computed via eq. (4).
(4) New values of $w(i)$ are computed using the following differential approximation:

$$w(i;\ t + \Delta t) = w(i;\ t) + \frac{dw(i)}{dt}\Delta t \qquad (6)$$

where the values of $dw(i)/dt$ are computed via eq. (2).

During the time course of the simulation the values of Δt and ω may be varied. Typically the initial value of Δt will be taken to be very small, and gradually increased over the first few hundred iterations to some maximal value, above which the numerical simulation becomes unstable due to failure of the differential approximations employed [1]. In a subsequent paper of this series an algorithm will be presented that permits the value of ω to be changed automatically in such a fashion as to maintain the concentration of CsCl at a predefined value at the bottom of the centrifuge tube.

3. Calculation of concentration-dependent hydrodynamic and thermodynamic properties of CsCl solutions

The sedimentation coefficient is a coefficient of proportionality between the force/unit mass exerted on a solute particle and the resulting steady-state velocity of the particle, and is given by [1]

$$s = \frac{M_w(1 - \bar{v}\rho)}{N f_s} \qquad (7)$$

[1] This "slow-start" procedure is used to eliminate instabilities that would otherwise arise from rapid, localized changes in solute concentration at the meniscus and base of the solution occurring at the outset of the simulation.

where M_w is the molar mass of solute [2], $\bar{v}$ the partial specific volume of solute, ρ the density of solution, N is Avogadro's number, and f_s the frictional coefficient for sedimentation.

The mutual diffusion coefficient is given by [1,2]

$$D = \frac{kT\nu}{f_d}(1 + w\ \mathrm{d}\ln\gamma/\mathrm{d}w) \tag{8}$$

where k is Boltzmann's constant, T is the absolute temperature, ν is the dissociation number (2 for CsCl), f_d the frictional coefficient for diffusion, and γ the thermodynamic activity coefficient, equal to $\gamma_\pm$ for electrolytes. The frictional coefficients for sedimentation and diffusion are equal in the limit of low solute concentration [1]. Although the two coefficients are, in principle, unequal at finite solute concentrations [3], they have been found to be identical to within experimental error for two different solutes, thallous sulfate [4] and sucrose [5] at concentrations up to 50 g/l. It will be assumed that the difference between the two quantities may be neglected for the present purpose, and we shall set

$$f = f_s = f_d \tag{9}$$

independent of CsCl concentration. This is the second major approximation underlying the present method of simulation, the validity of which is tested by comparing the results of simulations with experimental data.

Data have been reported for the dependence of D, ρ, and γ in CsCl solutions over a wide range of solute concentrations at 25 °C, but the concentration dependence of s has not. However, if the approximate relation eq. (9) is valid at all concentrations, then eq. (7) and (8) may be combined to yield

$$s = \frac{M_w(1 - \bar{v}\rho)D}{\nu RT(1 + w\ \mathrm{d}\ln\gamma/\mathrm{d}w)} \tag{10}$$

[2] Although cesium and chloride ions are dissociated in solution, they must sediment together to maintain electroneutrality and are consequently treated as a single effective species with $M_w = 168.4$ g/mol.

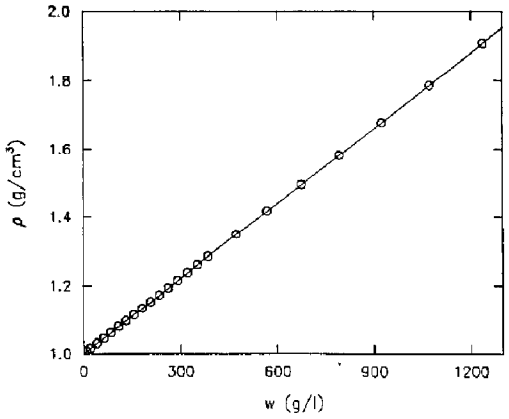

Fig. 1. Density of CsCl solution (25 °C) plotted as a function of w. Data points and curve described in text.

3.1 Density

The following linear equation was fitted by the method of least-squares to data taken from ref. [6]:

$$\rho(w) = \rho_0 + \rho_1 w \tag{11}$$

The data are plotted in Fig. 1 together with the dependence of ρ upon w calculated via eq. (11) with the best-fit parameter values $\rho_0 = 1.00047$, $\rho_1 = 7.34 \times 10^{-4}$.

3.2 Thermodynamic activity coefficient

The following semiempirical equation was fitted by the method of non-linear least squares to

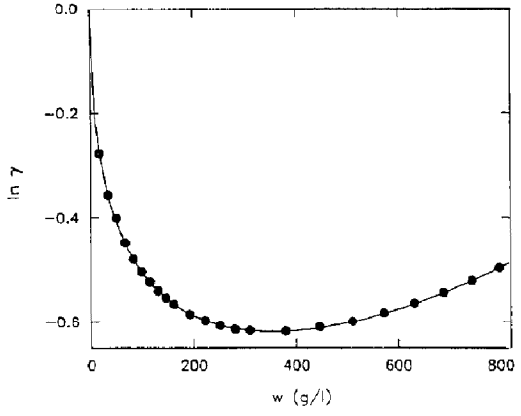

Fig. 2. Logarithm of the activity coefficient of CsCl (25 °C) plotted as a function of w. Data points and curve described in text.

data taken from Appendix 8.10 of ref. [2], converted from activity in molal units to activity in w/v concentration units (g/l):

$$\ln \gamma(w) = \frac{-B_0\sqrt{w}}{\left(1+B_1\sqrt{w}\right)} + B_2 w + B_3 w^2 \qquad (12)$$

The data are plotted in Fig. 2 together with the dependence of ln γ on w calculated via eq. (12) with the best-fit parameter values $B_0 = 8.16 \times 10^{-2}$, $B_1 = 4.56 \times 10^{-2}$, $B_2 = 5.43 \times 10^{-4}$, $B_3 = 1.23 \times 10^{-7}$. The derivative of ln γ with respect to concentration, employed in the calculation of s(w), is then given by

$$\frac{\mathrm{d} \ln \gamma(w)}{\mathrm{d}w} = \frac{-0.5B_0}{\sqrt{w}\left(1+B_1\sqrt{w}\right)^2} + B_2 + 2B_3 w \qquad (13)$$

3.3 Coefficient of mutual diffusion

The following empirical equation was fitted by the method of non-linear least squares to data taken from Appendices 11.1 and 11.2 of ref. [2]:

$$D(w) \times 10^5 = A_0 + (A_1 - A_0)\exp\left(-A_2 \frac{w}{\mathrm{M_w}}\right) + A_3 \frac{w}{\mathrm{M_w}} + A_4\left(\frac{w}{\mathrm{M_w}}\right)^2 + A_5\sqrt{\frac{w}{\mathrm{M_w}}} \qquad (14)$$

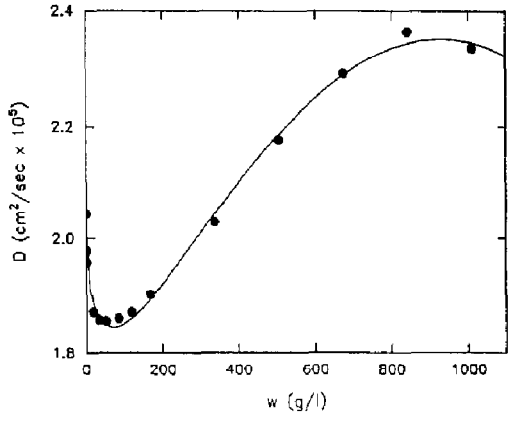

Fig. 3. Mutual diffusion coefficient of CsCl (25 °C) plotted as a function of w. Data points and curve described in text.

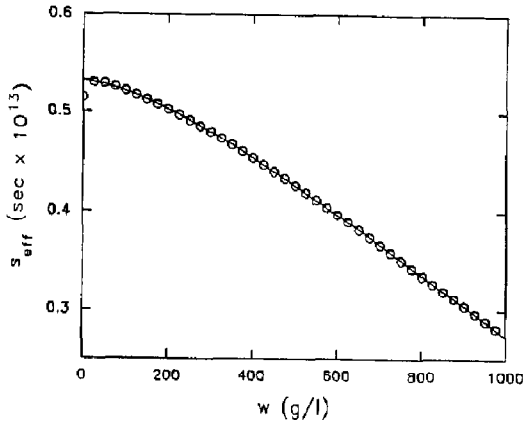

Fig. 4. Effective sedimentation coefficient of CsCl (25 °C) plotted as a function of w. Data points and curve described in text.

The data are plotted in Fig. 3 together with the dependence of D on w calculated using eq. (14) with the best-fit parameter values $A_0 = 2.04$, $A_1 = 2.03$, $A_2 = 18.1$, $A_3 = 0.507$, $A_4 = -3.41 \times 10^{-2}$, $A_5 = -0.614$.

3.4 Sedimentation coefficient

Using eqs. (10), (11), (13) and (14), the value of $s(w)$ was calculated for $w = 1, 26, 51, \ldots, 951, 971$ g/l. An empirical equation of the following form was fit by the method of non-linear least squares to the data in the resulting table excepting the three lowest concentration points:

$$s(w) \times 10^{13} = S_0 - S_1 w - S_2 \exp(-S_3 w) \qquad (15)$$

Points in the table are plotted in Fig. 4, along with the dependence of s upon w calculated via eq. (15) with the best-fit parameter values $S_0 = 5.96 \times 10^{-1}$, $S_1 = 3.22 \times 10^{-4}$, $S_2 = 6.33 \times 10^{-2}$, $S_3 = 3.99 \times 10^{-3}$.

3.5 Self-consistency of empirical representations

Equation (10) may be rewritten as

$$\mathrm{M_w} = \frac{s(w)\nu RT\left(1 + w\ \mathrm{d} \ln \gamma(w)/\mathrm{d}w\right)}{\left[1 - \bar{v}\rho(w)\right]D(w)} \qquad (16)$$

If the empirical functions for $s(w)$, d ln $\gamma(w)/\mathrm{d}w$, $\rho(w)$ and $D(w)$ are self-consistent and accurate, then the value of the expression on the right-hand

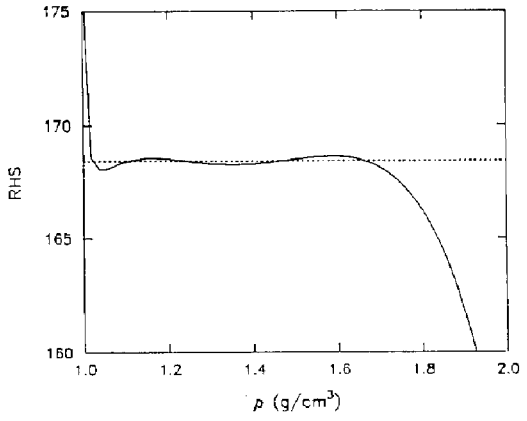

Fig. 5. Right hand side of eq. (16) plotted as a function of solution density.

side of eq. (16), which we will denote by RHS, calculated using these empirical functions, should be essentially independent of w and equal to M_w (168.4 g/mol) over the entire range of experimental data used to derive the empirical functions. This quantity is plotted against ρ in Fig. 5. It may be seen that RHS is within 4% of M_w for all $\rho \leq 1.90$, encompassing essentially the entire range of CsCl concentrations encountered experimentally. Since the data for ln γ extend only up to $\rho = 1.6$, and the data for D extend only to $\rho = 1.75$, the result presented here suggests that the empirical eqs. (12) and (14) provide reasonably accurate means for extrapolating these data to higher concentrations.

It should be noted that all values of thermodynamic and hydrodynamic data refer to values measured at atmospheric pressure. It is assumed that these values are valid semiquantitatively at the higher pressures found within the solution centrifuged at high angular velocities [7].

4. Equilibrium CsCl gradients

At sedimentation equilibrium the condition of constant chemical potential of solute throughout the solution may be expressed as [1]

$$\left(\frac{d\mu}{dw}\right)_{P,T} \cdot \frac{dw}{dr} = M_w(1-\bar{v}\rho)\omega^2 r \tag{17}$$

where μ is the chemical potential of solute. For dissociable solutes, the chemical potential is expressed as

$$\mu = \mu^o + \nu RT \ln \gamma w \tag{18}$$

where ν is the dissociation number. Equations (17) and (18) may be combined to yield

$$\frac{dw}{dr} = \frac{M_w(1-\bar{v}\rho)\omega^2 rw}{\nu RT[1 + w \, d \ln \gamma/dw]} \tag{19}$$

Equilibrium gradients for a prespecified value of the loading concentration of CsCl, denoted by w_L, were calculated in an iterative fashion as follows. For iteration j an estimate is made of the value of $w(n+1) = w_{base}^{(j)}$ is made. The values of ρ and $d \ln \gamma/dw$ are calculated for this concentration using eqs. (11) and (13) respectively. Then the value of dw/dr for $r = r(n+1)$ is calculated using eq. (19). The value at $r(n)$ is calculated using the linear approximation

$$w(i-1) = w(i) - \left(\frac{dw}{dr}\right)_{r=r(i)} \Delta r \tag{20}$$

This calculation is repeated for successively smaller i down to $i = 1$. The average concentration is then calculated using

$$w_{av}^{(j)} = \sum_{i=1}^{n} w(i)V(i) / \sum V(i) \tag{21}$$

and compared to the prespecified loading concentration. The value of w_{base} to be used in the next iteration is then calculated via

$$w_{base}^{(j+1)} = w_{base}^{(j)} w_L / w_{av}^{(j)} \tag{22}$$

The entire procedure is repeated iteratively until $w_{av}^{(j)}$ approaches w_L to within some prespecified criterion of convergence, typically 1 part per thousand.

Equation (19) is entirely thermodynamic in origin. The condition of sedimentation equilibrium may also be expressed in hydrodynamic terms by setting the value of the flux J in eq. (1) equal to zero for all values of r. Then combination of eqs. (1), (7) and (8) yields

$$\frac{dw}{dr} = \frac{M(1-\bar{v}\rho)\omega^2 rw}{\nu RT[1 + w \, d \ln \gamma/dw]} \frac{f_d}{f_s} \tag{23}$$

which is identical to eq. (19) if it is assumed that $f_d = f_s$. Thus the approximate eq. (9), introduced in the previous section to facilitate calculation of the effective sedimentation coefficient as a function of concentration, may be seen to lead to a thermodynamically correct formulation of the concentration gradient in the limit of long time.

5. Comparison of simulated and experimental results

5.1 Formation of an equilibrium gradient

The following experiment was performed by O.M. Griffith (Beckman Instruments, Spinco Division). A solution of CsCl having initial uniform loading density $\rho_L = 1.50$ g/cm^3 was centrifuged to equilibrium (25 °C) at a rotor speed of 40,000 rpm in a Beckman Model E analytical ultracentrifuge. The refractive index gradient was monitored and recorded at regular intervals of elapsed time by means of calibrated Schlieren optics. The Schlieren patterns were numerically integrated to yield the absolute concentration of CsCl as a function of time and position within the sector-shaped cell.

This experiment was simulated via the procedure described above. Instead of attempting to replicate the (unknown) rotor acceleration protocol, it was assumed that the distribution of solute when the rotor reached its final velocity would be equivalent to that obtained by an application of force at the final rotor velocity for a (shorter) period of elapsed time, that would result in the same value of $\int \omega^2 t$. Elapsed times of the simulation were therefore reduced by 5 min to reflect this correction. The results of the simulation are plotted together with the previously unpublished experimental data of Griffith in Fig. 6.

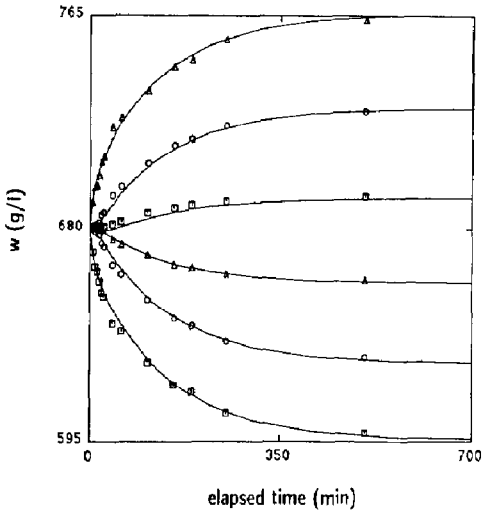

Fig. 6. CsCl concentration as a function of time at selected radial positions in a sector-shaped cell. Experimental conditions are given in the text. Points: unpublished data of O.M. Griffith. Curves: results of simulation conducted as described in text, with $n = 50$. Sets of data points and associated curves, plotted from top to bottom of the figure, correspond to the following radial positions: 7.17, 6.90, 6.64, 6.37, 6.11, and 5.84 cm, respectively.

5.2 Decay of previously formed equilibrium gradient

The following experiment was reported by Ifft et al. [8]. A CsCl solution ($\rho_L = 1.700$) was centrifuged to sedimentation equilibrium at 39,460 rpm in a Beckman Model E. Over a period of 6 minutes the rotor velocity was then reduced to 9,945 rpm, and a series of schlieren photographs were made to monitor the decay of the initial gradient.

This experiment was simulated by calculating the equilibrium concentration gradient of CsCl at 39,460 rpm, as described above, and setting the calculated gradient equal to the initial gradient in the simulation. The initial rotor velocity was set to 39,460 rpm, reduced at a constant rate so as to reach a final velocity of 9,945 rpm at a simulated elapsed time of 6 minutes, remaining at the final velocity thereafter for the duration of the simulation. The results of the simulation are presented in Fig. 7, together with experimental data points obtained by digitization of Fig. 9 of Ifft et al. [8].

5.3 Formation of an equilibrium gradient in a fixed-angle rotor

The following experiment was performed by A. Furst (Beckman Instruments, Spinco Division). Aliquots of a solution of CsCl of density $\rho_L = 1.205$ g/cm^3 were loaded into several Quickseal

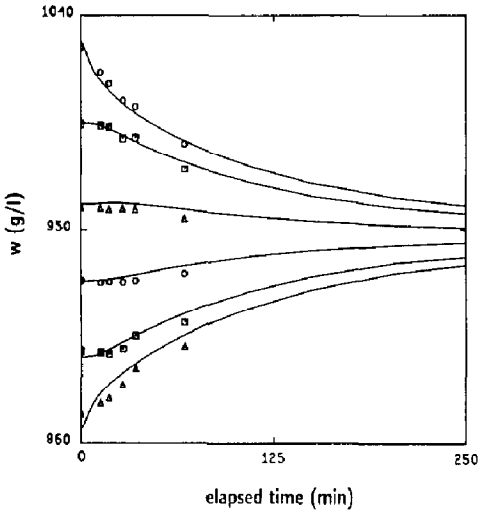

Fig. 7. CsCl concentration as a function of time at selected radial positions in a sector-shaped cell. Experimental conditions are given in the text. Points: data of Ifft et al. [8]. Curves: results of simulation conducted as described in text, with $n = 50$. Sets of data points and associated curves, plotted from top to bottom of the figure, correspond to the following radial positions: 7.18, 6.93, 6.67, 6.42, 6.16, and 5.91 cm, respectively.

(TM) centrifuge tubes and centrifuged at 75,000 rpm and 25° C for different lengths of time in a 75Ti fixed-angle rotor, in which the cylindrical axis of the centrifuge tube lies at an angle of 25.5° to the axis of rotation. After the conclusion of centrifugation, the rotor was brought to a halt via coasting, the tubes removed, and between 18 and 22 fractions per tube collected via tube puncture. The refractive index of each fraction was determined with an Abbé refractometer, and the average concentration of CsCl in the fraction calculated therefrom using standard tables.

This experiment was simulated using the one-dimensional model described above. The geometry of the centrifuge tube in the rotor (i.e., cross-section as a function of radial distance) was projected onto the radial direction in order to test the assumption that net motions of solute species in directions other than than the radial direction may be neglected to a first approximation. From the geometry of the tube in the rotor one may calculate the total volume within the tube that is inside a given radial distance r, $V(r)$. It is assumed that as the rotor coasts to a halt, and the tube removed from the rotor, the laminar region of solution normal to the radial direction lying at r^* in the presence of the field will reorient such that it will be found at a volume $V(r^*)$ relative to the top of the centrifuge tube oriented vertically, and that minimal mixing will occur between the contents of adjacent laminae. No attempt was made to simulate rotor acceleration or deceleration.

The previously unpublished data of Furst are shown together with results of the simulation in Fig. 8. In view of the simplifying approximations inherent in the simulation, the extent of agreement between experimental and simulated gradients is remarkable. The discrepancy between simulation and data is largest for the longest duration of centrifugation (71 h), corresponding to an equilibrium gradient in the context of the simulation. Since the equilibrium gradient is in principle independent of the shape of the centrifuge cell, wall effects do not account for the discrepancy, which is attributed to a combination of partial failure of the reorientation approximation described above, partial decay of the gradient during rotor deceleration and subsequent fractionation, and neglect of the effect of hydrostatic pressure on thermodynamic activity.

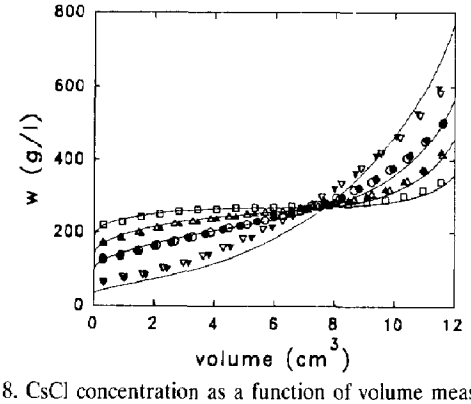

Fig. 8. CsCl concentration as a function of volume measured from the top of a Quickseal (TM) centrifuge tube. Symbols represent the data of Furst for the following durations of centrifugation: 2 hours (□); 5 hours (△,▲); 10 hours (○,●); 71 hours (▽,▼). Curves represent the results of simulations carried out as described in the text.

6. Discussion

There exists a considerable body of literature, reviewed in ref. [9], dealing with numerical solutions to the one-dimensional sedimentation-diffusion equation. We are aware of only one previous published method [10] for the simulation of the dynamics of the formation of density gradients that takes into account extreme deviations from thermodynamic ideality. While the physico-chemical concepts underlying the two approaches are similar, considerably simpler physical and mathematical approximations are used in the present implementation to facilitate rapid real-time simulation using inexpensive personal computers [3]. Comparison with experiment indicates that results obtained using the computational procedures and approximations presented here are sufficiently realistic to be useful in the design of experiments. Further elaboration and demonstration of the utility of this approach will be presented in the following papers of this series.

[3] A program written in Turbo Pascal, with $n = 50$, models density gradient formation at actual speeds over one-hundred fold faster than the simulated elapsed time (i.e., 1 minute simulation time is ca. 2 h simulated elapsed time), when running on an 8 MHz 80286 AT-compatible microcomputer equipped with 80287 math coprocessor.

Acknowledgements

This work was supported in part by Beckman Instruments, Spinco Division, to whom thanks are given for permission to present the heretofore unpublished results of O.M. Griffith and A. Furst. Special thanks are given to J.C. Osborne, Jr., Beckman Instruments, for proposing this study and encouraging its development, and to J. Marque, Beckman Instruments, for careful reading and critical review of the manuscript.

References

1 C. Tanford, Physical chemistry of macromolecules (Wiley, New York, NY, 1961).
2 R.A. Robinson and R.H. Stokes, Electrolyte solutions (Academic Press, New York, NY, 1959).
3 J.L. Anderson, Ind. Eng. Chem. Fundam. 12 (1973) 488.
4 J.M. Creeth, J. Phys. Chem. 66 (1962) 1228.
5 F.E. Labar and R.L. Baldwin, J. Am. Chem.Soc. 85 (1963) 3105.
6 International Critical Tables, Vol. 3 (McGraw-Hill, New York, NY, 1928) 94.
7 J.E. Hearst, J.B. Ifft and J. Vinograd, Proc. Natl. Acad. Sci. U.S.A. 47 (1961) 1015.
8 J.B. Ifft, D.H. Voet and J. Vinograd, J. Phys. Chem. 65 (1961) 1138.
9 H. Fujita, Foundations of Ultracentrifugal Analysis (Wiley, New York, NY, 1975).
10 W.K. Sartory, H.B. Halsall and J.P. Breillatt, Biophys. Chem. 5 (1976) 107.